

Geometric Structures in mesoscale urban flows

Halios C.H.^{1*}, Helmis C.G.², Asimakopoulos D.N.²

¹University of Reading, Department of Meteorology

² National and Kapodistrian University of Athens, Faculty of Physics, Department of Environmental Physics and Meteorology

*corresponding author:

e-mail: c.halios@reading.ac.uk

Abstract Geometric structures with the shape of waves, ramp, cliff, and step changes are commonly observed in a wide range of temporal signals such as meteorological or energy production time series. Traditionally, geometric shapes found in turbulence were examined in the context of coherent structures; they are believed to dominate the turbulent energy and mass exchange within the atmospheric boundary layer during surface-layer plumes or mixed-layer thermals. More recently, meteorological geometric structures have been associated with low-dimensional chaotic systems; in energy production time series, geometric structures are associated with significant energy losses. In this study a simple linear technique is used to extract geometrical shapes from datasets that were measured at a suburban location experiencing a number of different mesoscale modes. General characteristics of the atmospheric fields were examined by applying Principal Component Analysis and Integral Statistics as an objective measure of air mass stagnation, recirculation and ventilation. Certain geometric structures were found to be associated with particular flows: e.g. temperature positive cliff-ramps and ramp-cliffs appear mainly during night time and under weak flow fields. This study discusses new methods based on single station common meteorological measurements that enhance our understanding of complex processes. These methods are directly applicable to a wide range of fundamental and applied science areas.

Keywords: Urban, mesoscale, structures, geometric shapes

1. Introduction

Geometric shapes of coherent structures such as ramp or cliff like signals, step changes and waves in meteorological temporal series, are commonly observed during atmospheric measurements. Scientific interest on coherent structures was intensified after a number of studies indicated that they might dominate the turbulent energy and mass exchange between the atmospheric surface layer and the layers above (e.g. Gao *et al.*, 1989; Serafimovich *et al.*, 2011). Also, from a theoretical point of view it was proposed recently that, under the presence of large organized structures, highly complex atmospheric turbulent flows start behaving as low dimensional chaotic systems (Campanharo *et al.*, 2008, Wesson *et al.*, 2003).

The existence of ramp like structures in turbulence is well established and measured in field and laboratory experiments (Taylor, 1958; Barthlott, 2008; Serafimovich *et al.*, 2011). A variety of conditional sampling techniques have been developed in order to objectively identify structural shapes in meteorological time series, and often contradictory interpretations of results obtained with different methods are reported (Krusche and deOvileira (2004) and references therein). Belucic and Mahrt 2012 (BM2012 hereafter) introduced a simple linear technique to extract geometrical shapes that are usually observed in small scale turbulence and in meso-scale flows. They applied the technique to temperature and wind speed time series measured at Kutina, Croatia, for different scales (from 3s up to 2h: thus covering a wide range of the turbulent and meso-scales). They found a minimum in the number of recognized structures at time scales between 2 and 10 minutes in accordance with the known minimum of kinetic energy between turbulence and mesoscales. They also proposed that the relationships between the basic geometrical shapes are independent of the scale under consideration, despite the changing physics.

In this work the same technique described above has been applied on a dataset which had been obtained at a location experiencing a number of different mesoscale modes (Helmis *et al.* 1995; Helmis and Papadopoulos, 1996; Kallos, 1993). The aim of this work is to extract the geometrical characteristics of the one hour time scales and then to relate the extracted structures with aspects of the mesoscale flows.

2. Methods

2.1. Experimental Site

In the present work, the Automatic Meteorological Station (AMS) of the Lab of Meteorology of the Physics Department, University of Athens which is located at the University Campus on the eastern foothills of Hymettus mountain, 5 km from the city center, was used. (Figure 1). The experimental site as well as the instrumentation used are analytically described in Halios *et al.*, 2012. For the present study we used a dataset of 1 min measurements of atmospheric pressure (P, hPa), temperature (T, C), relative humidity (RH, %), solar radiation (SR, W m⁻²), wind speed and direction (WS and WD, ms⁻¹, degrees

respectively) measured at 10m and wind shear between 10 m and 5 m agl, for the time period 11/1/2000–23/5/2000.

2.2. Geometric Structures

In the following, the basic steps of the methodology employed for the identification of geometric structures are briefly described. Full details of the methodology can be found in BM2012.

(a) Initially four basic geometric shapes were chosen:

- a ramp-cliff function (gradual rise in time series followed by a sudden drop),
- a cliff-ramp function (or a reversed ramp-cliff: sudden rise followed by a gradual drop),
- a step function and
- a simple sine function.

Each shape can have two orientations: the shape can start with a positive or negative gradient ($\theta/\theta t$); thus we end up with eight shapes which are used for further analysis (see Figures 6 and also Figure 2 in BM2012.). Consequently 8 time series each of 60 data points were created, each one corresponding to one of the eight pre-defined structures.

(b) Each geometric shape of 60 data points move step-by-step through the time series under consideration (wind speed and temperature) and for each location (consisting of 60 points) the correlation coefficient is calculated. Parts with 60 points (minutes) in the time series which have a correlation coefficient >0.9 with the pre-selected shape are selected and categorized under the specific structure; for the step and sine structures extra filters are applied, in order to avoid misinterpretation.

(c) the part of the time series that was just recognized as being part of the specific shape is deleted, and excluded from further analysis.

(d) The procedure for the specific shape is completed after all parts with $r>0.9$ have been selected.

(e) the procedure begins for the next geometric shape.

2.3. Mesoscale Flows

The characteristics of the meso-scale flows and general meteorological conditions were studied using two methodologies: (1) a Principal Component Analysis (PCA) for the determination of the dominant surface patterns which was previously applied to a wider dataset from the same location and (2) an analysis of the so-called Integral quantities which are used to characterize stagnation, recirculation and ventilation conditions (Allwine and Whiteman, 1994). The following variables have been used for PCA: T- temperature ($^{\circ}\text{C}$) at 10 m a.g.l., RH- Relative Humidity (%) at 10 m a.g.l., WDsd- standard deviation of the hourly Wind Direction (degrees) at 10 m a.g.l., Vsd- standard deviation of the hourly wind speed (m s^{-1}) at 10 m a.g.l., absu- the absolute value of the across the mountain axis component of the wind speed (m s^{-1}), absv- the absolute value of the along the mountain axis component of the wind speed (m s^{-1}), shear- the wind shear between 10 m and 5 m a.g.l.

3. Results

Three PCs accounting for 77.4 % of the total variance were rotated with varimax Rotation, and are interpreted according to the values of the respective loadings. PC2 contrasts temperature and solar radiation to humidity (correlation coefficients 0.81, 0.72 and -0.77, respectively). The other two PCs (PC1 and PC3, respectively) are related with the along (v) and across (u) axis mountain components of the wind speed. PC1, (related to the along-mountain wind speed component, correlation coefficient 0.91) is also highly correlated with intense changes in the wind speed ($R = 0.89$) and wind shear ($R = 0.84$); thus it is related with mechanically generated turbulence. Finally PC3 is related mainly with the u-component of the wind speed ($R = 0.96$), and also moderately correlated with intense changes in the wind speed ($R = 0.32$) and shear ($R = 0.33$). Similar results were found in Halios *et al.*, 2012.

Analysis of the integral quantities showed that out of the 2294 cases, 25% were categorized as ventilation conditions, 7% as recirculation conditions and 3% as stagnant conditions. The remaining 65% of the cases do not belong to any of these categories, thus they are categorized as intermediate conditions. The large percentage of the intermediate conditions is probably related to the strong terrain which leads to highly variable flows. In Figures 2a and 2b, the percentage of occurrences of recognized structures in the temperature and wind fields is presented. The percentage of occurrences is the number of structures identified for each category divided by the maximum number of possible events in the data set. One striking difference between the two datasets is that the temperature field appears much better organized than the wind speed. In particular, all wind speed structures are less than 1% of the maximum theoretical number of events; the percentage is higher than 1% for all temperature structures. Following BM2012 we propose that pressure fluctuations and shear instabilities act to smooth out the large momentum gradients, thus leading to less shapes in the wind speed field than in the temperature field. Percentage of (positive or negative) sine and step shapes are always higher than the corresponding percentage of (positive or negative) ramp-cliff or cliff-ramp shapes, again in accordance with BM2012. A striking exception is the large percentage of positive cliff-ramp shapes in the temperature field, where 3.1% of the maximum theoretical number of events are cliff-ramp shapes against 1%, 1.3% and 1.4% for ramp-cliff, step and sine shapes respectively. It has been proposed in several studies that within the turbulence scales, the preference of some specific geometric shapes is related with certain physical mechanisms, e.g. ramp and cliff structures in the temperature field are related with sharp asymmetrical thermals and/or intermittent turbulence in stable conditions, whilst sines are related with smooth wave-like motions in the stable boundary layer (e.g. BM2012). For the larger scales as the one discussed here, the reason for the dominance of some shapes against the others is not quite clear. Yet, it is perhaps of interest to notice that for turbulence scales, cliff-ramp shapes with positive gradient are usually observed under stable conditions (Barthlott *et al.*, 2007); and in our study the large percentage of these cases is observed during night time (see next section). This perhaps indicates to the development of this particular type of stratification in this environment.

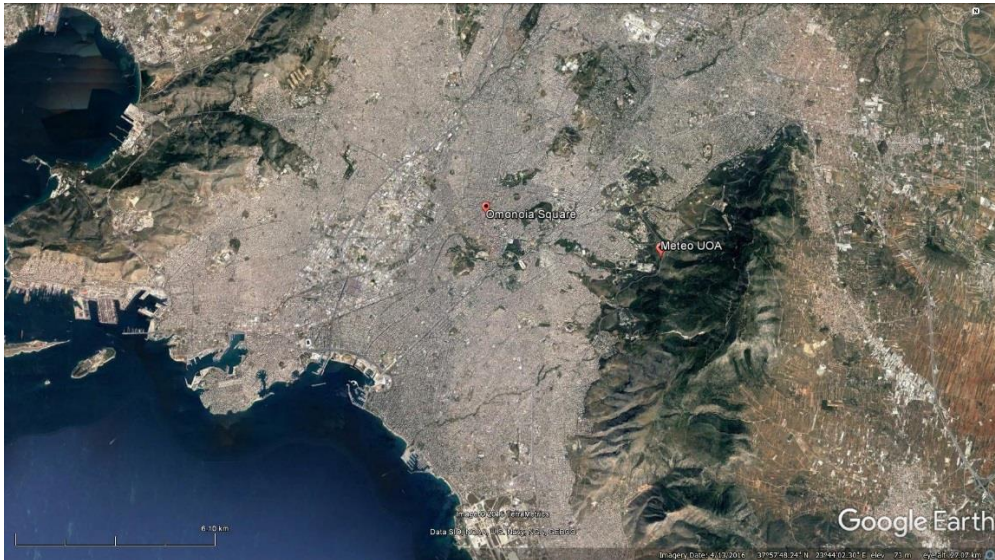


Figure 1. The Greater Athens Area. In the map the location of the university campus (Meteo UOA) and the center of the city (Omonoia Square) are denoted.

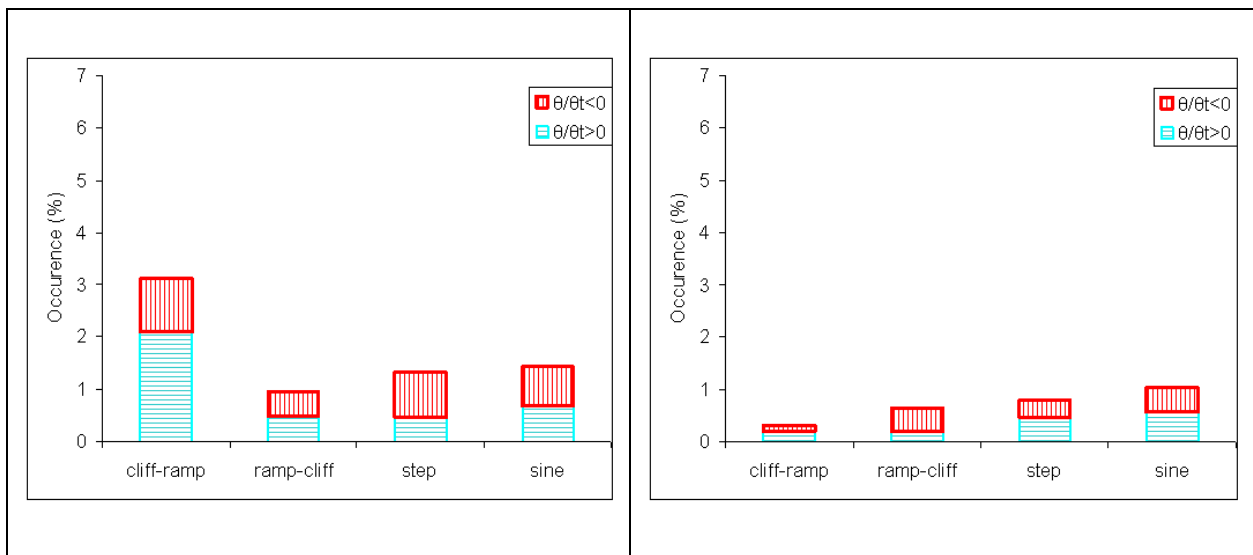


Figure 2. The percentage of recognized temperature (a) and wind speed (b) events relative to the theoretically maximum number of events.

At Tables 1 and 2 the percentage of the identified shapes (separated in positive and negative gradients) is presented according to the day period (night-time or day-time), the status of the flow field (ventilation, stagnation, recirculation or intermediate) and the dominant surface pattern (Principal Component Scores).

For the temperature structures (Table 1), mixed conditions are observed in terms of the flow fields and dominant surface pattern; several structures are under ventilation conditions, some under recirculation conditions and only a few under stagnant conditions.

The ramp-cliffs with negative gradient are observed under several recirculation conditions which in turn are related to enhanced along-mountain wind speed. For the turbulence scales this structure is associated with unstable conditions (Barthlott *et al.*, 2007); contrary to this, in our study this structure is related with negative PC2 scores which occur either during night time, or under low pressure systems and fronts (Halios *et al.*, 2013). 52% of these cases occur during night time. Thus, it is apparent that in the mesoscale region this particular structure is not related with the same physics that dominates turbulence scales.

Table 1. Statistics of the identified temperature shapes according to the day period, status of the flow field and the dominant surface pattern

day/night (%)		conditions (%)						PC scores (%)			PC scores (median)		
		Day	night	rec	stag	vent	inter	PC1	PC2	PC3	PC1	PC2	PC3
c-r	p	24	76	11	6	28	55	43	2	43	-0.17	-0.38	-0.17
	n	48	52	4	7	26	63	30	48	41	-0.47	-0.03	-0.32
r-c	p	0	100	0	0	25	75	33	42	25	-0.47	-0.37	-0.64
	n	50	50	33	0	33	33	67	17	33	0.28	-0.32	-0.23
Step	p	67	33	8	8	33	50	17	42	17	-0.69	-0.11	-0.22
	n	39	61	5	0	21	74	47	53	47	-0.09	0.03	-0.01
Sine	p	50	50	13	0	13	73	33	40	60	-0.21	-0.24	0.31
	n	60	40	6	0	35	59	59	53	29	0.47	0.28	-0.26

p: positive ($\theta/\theta_t > 0$), n:negative ($\theta/\theta_t < 0$)

Table 2. Statistics of the identified wind speed shapes according to the day period, status of the flow field and the dominant surface pattern

day/night (%)		conditions (%)						PC scores (%)			PC scores (median)		
		Day	night	rec	stag	vent	inter	PC1	PC2	PC3	PC1	PC2	PC3
c-r	p	40	60	0	0	0	100	0	50	0	-1.12	0.08	-0.52
	n	0	100	0	50	0	50	0	50	0	-1.76	-0.19	-0.64
r-c	p	20	80	0	0	25	75	0	75	25	-0.72	0.40	-0.97
	n	0	100	0	0	0	100	0	33	33	-1.35	-0.59	-0.36
Step	p	25	75	10	10	0	100	0	50	10	-1.48	0.03	-0.70
	n	11	89	5	0	21	74	13	38	38	-1.08	-0.58	-0.20
Sine	p	15	85	0	0	0	100	15	15	15	-0.55	-0.74	0.53
	n	0	100	9	9	9	73	9	18	9	-0.83	-0.65	-0.46

p: positive ($\theta/\theta_t > 0$), n:negative ($\theta/\theta_t < 0$)

Cliff-ramp with positive gradients and ramp-cliff with negative gradients are related with stable conditions in turbulence scales (Barthlott *et al.*, 2007). Here, these structures appear mainly during night time (76% and 100% of the cases respectively), and correspond to negative PC1 and PC3 scores, indicating a weak flow field. This is especially true for the ramp-cliffs with a positive gradient (100% of the cases occur in night), which are observed under the total absence of recirculation conditions. It can be seen that there is a percentage of positive PC1 and PC3 scores (33% and 25% for PC1 and PC3 respectively) under temperature positive ramp-cliffs, which correspond to ventilation conditions. It is perhaps surprising that there are no stagnation conditions under this category; the very high percentage of unrecognized flows during this category could be an indication of the sensitivity of the method to the strong mountainous terrain. Further investigation of this issue would be of interest, but it is outside the scope of this article. Positive step and negative sine shapes tend to appear during day time and they are related with enhanced ventilation values. Negative step and positive sine structures don't show a clear preference for the period of

day, the flow or the temperature pattern. Exception to this, is the positive sine shape for which the ventilation cases are few and are related with the across mountain wind speed and low SR and T values, indicating weak local flows that develop during night time. In contrast to the results of the temperature structures, it is apparent that uniform weak conditions dominate across all the wind structures (Table 2). The vast majority of the wind speed structures appears during night time, and consequently are related to negative PC2 score. They are also occurring under calm conditions (high negative PC1 and PC3 scores): it is characteristic that out of the 64 detected cases only one structure was observed under ventilation conditions. This is in line with the situations observed elsewhere in turbulent scales (e.g. BM2012). An exception is the positive step shapes, where some cases were observed under recirculation conditions

4. Conclusions

A recently developed simple linear technique, for the detection of basic shapes in meteorological time series was

applied in the wind speed and temperature data of the time scale of 1h measured at a location where a wide range of meso-scale flows have been identified in the past. Step changes, cliff-ramp, ramp-cliff and wave-like signals were identified, and it was found that the temperature field appears much better organized than the wind field. Cliff-ramp structures are dominant in the temperature time series.

The occurrence of structural shapes was related with the dominant flow patterns by applying Principal Component Analysis and analysis of integral quantities (wind run and recirculation factor) to the data. As integral quantities are true measures of the transport of a plume only under idealized homogeneous wind conditions it was argued that for this reason the large portion of flow conditions was not categorized. Nevertheless, 25% of the cases were categorized as ventilation conditions, 7% as recirculation and only 3% as stagnant conditions.

The temperature positive cliff-ramps and ramp-cliffs that within turbulence scales are related with stable conditions appear mainly during night time and under weak flow field. Temperature step and sine structures don't show a clear preference for the period of day, flow or temperature pattern. On the contrary, uniform stable, weak flow conditions dominate across all the wind speed structures.

References

- Allwine K.J. and Whiteman C.D. (1994), Single-station integral measures of atmospheric stagnation, recirculation and ventilation, *Atmospheric Environment*, **28**(4), 713-721.
- Barthlott, C., P. Drobinski, C. Fesquet, T. Dubos, and C. Pietras (2007), Long-term study of coherent structures in the atmospheric surface layer, *Boundary-Layer Meteorology*, **125**, 1–24.
- Belušić D. and Mahrt L. (2012), Is geometry more universal than physics in atmospheric boundary layer flow?, *Journal of Geophysical Research*, **117**, D09115, doi:10.1029/2011JD016987, 2012.
- Campanharo, A. S. L. O., Ramos F. M., Macau E. E. N., Rosa R. R., Bolzan M. J. A., and A Sá L. D. (2008), Searching chaos and coherent structures in the atmospheric turbulence above the Amazon forest, *Philos. Trans. R. Soc. A*, 366, 579–589.
- Gao, W., R. H. Shaw, and R. T. Paw U (1989), Observation of organized structure in turbulent flow within and above a forest canopy, *Boundary-Layer Meteorology*, **47**, 349–377.
- Halios C.H., Helmis C.G., Flocas H.A., Nyeki S., Assimakopoulos D.N. (2012), On the variability of the surface environment response to synoptic forcing over complex terrain: a multivariate data analysis approach, *Meteorology and Atmospheric Physics* **118** (3-4), 107-115.
- Helmis C.G., K.H. Papadopoulos, (1996), Some aspects of the variation with time of Katabatic flow over a simple slope, *Quarterly Journal of the Royal Meteorological Society*, **122** (531), 595-610.
- Helmis C.G., Papadopoulos K.H., Kalogiros J., Soilemes A.T. and Assimakopoulos D.N. (1995), The influence of the background flow on the evolution of the Saronic Gulf Sea Breeze, *Atmospheric Environment*, **29** (24), 3689-3701.
- Kallos, G., P. Kassomenos, and R.A. Pielke, 1993: Synoptic and mesoscale weather conditions during air pollution episodes in Athens, Greece. *Boundary-Layer Meteorol.*, 62, pp. 163-184.
- Krusche N. and De Oliveira A.P. (2004), Characterization of coherent structures in the atmospheric surface layer, *Boundary-Layer Meteorology* **110**, 191–211.
- Serafimovich A., Thomas C., Foken T. (2011), Vertical and Horizontal Transport of Energy and Matter by Coherent Motions in a Tall Spruce Canopy, *Boundary-Layer Meteorology*, **140**, 429–451.
- Taylor, R. J. (1958), Thermal structures in the lowest layers of the atmosphere, *Australian Journal of Physics*, **11**, 168–176.
- Wesson, K. H., Katul G. G., and Siqueira M. (2003), Quantifying organization of atmospheric turbulent eddy motion using nonlinear time series analysis, *Boundary Layer Meteorology*, **106**, 507–525.